Journal of Solid Mechanics Vol. 6, No. 1 (2014) pp. 1-18

Vibration and Bifurcation Analysis of a Nonlinear Damped Mass Grounded System

M. Mostoufi, H. Nahvi *, B. Mirshafiee

Department of Mechanical Engineering, Isfahan University of Technology, Isfahan 8415683111, Iran

Received 1 September 2013; accepted 17 November 2013

ABSTRACT

In this paper, vibrations and bifurcation of a damped system consists of a mass grounded by linear and nonlinear springs and a nonlinear damper is studied. Nonlinear equation of motion is derived using Newton's equations. Approximate analytical solutions are obtained using multiple time scales (MTS) method. For free vibration, the approximate analytical results are compared with the numerical integration results. Forced vibrations of the system in primary and secondary resonant cases are studied and the effects of different parameters on the frequency-responses are investigated. Moreover, bifurcation of the system is studied considering different control parameters.

Keywords: Nonlinear vibration; Mass grounded system; Multiple time scale; Bifurcation

1 INTRODUCTION

A MECANICAL system with single degree-of-freedom including linear and nonlinear springs in series has technical applications. When in a system linear springs are connected to each other in series or parallel, they can be easily replaced by their equivalents [1, 2]. Sometimes one of the springs in parallel may be linear while the other is nonlinear. This system is named mass grounded system. This case results in an equivalent nonlinear spring which has a larger coefficient for its linear portion. On the other hand, if a linear spring is connected with a nonlinear one serially, obtaining an equivalent spring becomes complicated. In order to find a better insight into the behavior of such a system, some researchers tried to find its behavior.

Telli and Kopmaz [3] derived the equation of motion of a mass grounded system with linear and nonlinear springs in series and found an approximate periodic solution using the Linstedt–Poincare (LP) and the classical Harmonic Balance (HB) methods. They showed that the obtained analytical solution, depending on initial deflection of nonlinear spring, may have large deviations from numerical solution. Sun and Wu [4] explained that this difference is occurred because the LP method applies to a weakly nonlinear system and also the HB method is applicable under special assumptions. They also studied mass grounded systems in both hardening and softening spring cases and stabilized a qualitative analysis to find various singular points. They found that these systems have symmetric and asymmetric oscillation, depending on the value of system parameters. Wu and Li [5] proposed a linearized harmonic balance to obtain approximate analytical periods for a class of nonlinear oscillators. Lai and Lim [6] applied the method of Wu and Li to the mass grounded systems.

In this paper, vibration analysis of a mass-grounded system including linear and nonlinear springs and a nonlinear damper is carried out using multiple time scales method. Forced vibrations of the system in primary and secondary resonances are studied and the effects of different parameters on the frequency-response are investigated.

* Corresponding author. Tel.: +983113915242; Fax: +983113912628.
E-mail address: hnahvi@cc.iut.ac.ir (H. Nahvi).

Moreover, bifurcation of the system is studied using different control parameters. To the authors' knowledge, damping and bifurcation analysis of nonlinear mass grounded systems has not been reported yet.

2 EQUATIONS OF MOTION

Consider the mass-grounded system shown in Fig. 1 in which linear and nonlinear springs in series and a nonlinear damper are connected to a mass. In this system, k_1 is the stiffness coefficient of the linear spring and k_2 and k_3 are the linear and nonlinear stiffness coefficients of the nonlinear spring. Also c_2 and c_3 are the linear and nonlinear damping coefficients of the damper. Let y_1 and y_2 denote absolute displacements of the mass and the connection point of the two springs, respectively. Equations of motion of the system may be written as:

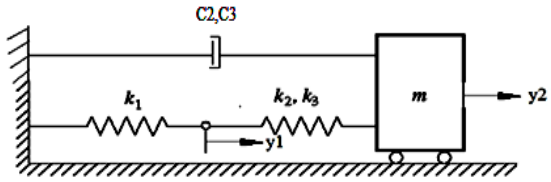

Fig. 1
A mass-grounded system with springs and a nonlinear damper.

$$K_1 y_1 = K_2 u + K_3 u^3 \tag{1}$$

$$m\ddot{y}_2 + c_2 \dot{y}_2 + c_3 \dot{y}_2^{\,3} + K_2 u + K_3 u^3 = 0 \tag{2}$$

where $y_2 - y_1 = u$

Equations of motion can be reduced to a single non-dimensional equation as:

$$\ddot{u} + \varepsilon\mu\dot{u} + \omega_0^{\,2} u + \varepsilon(6\lambda\eta u\dot{u}^2 + 3\lambda\eta u^2\ddot{u} + \lambda\omega_0^{\,2} u^3 + \mu\beta\delta\dot{u}^3) = 0 \tag{3}$$

where

$$\xi = \frac{k_2}{k_1}, \omega_0^{\,2} = \frac{k_2}{m(1+\xi)}, \varepsilon = \frac{k_3}{k_2}, \eta = \frac{\xi}{1+\xi}, \omega\mu = \frac{c_2}{m}, \delta = (1+\xi)^2 = (\frac{1}{1-\eta})^2, \beta = \frac{c_3}{c_2}$$

In this study, a parameter λ is added to the governing equation of motion (3) to show the hardening and softening cases.

3 FREE VIBRATIONS

3.1 Analytical solution

Multiple time scales method is used to solve Eq. (3). Two term expansion of u in MTS method is used as [7]:

$$u = u_0 + \varepsilon u_1 \tag{4}$$

and time scales as:

$$T_0 = t, T_1 = \varepsilon t \tag{5}$$

The first and second derivatives of u with respect to time t would be:

$$\frac{du}{dt} = \frac{\partial u}{\partial T_0} + \varepsilon \frac{\partial u}{\partial T_1} = \left(D_0 + \varepsilon D_1\right)u \tag{6a}$$

$$\frac{d^2u}{dt^2} = \frac{\partial^2 u}{\partial {T_0}^2} + 2\varepsilon \frac{\partial^2 u}{\partial T_0 \partial T_1} + \varepsilon^2 \frac{\partial^2 u}{\partial {T_1}^2} = \left(D_0^2 + 2\varepsilon D_0 D_1\right)u \tag{6b}$$

Substituting Eqs. (4) - (6) into Eq. (3) and equalling the same coefficients of ω^0 and ω^1 to zero yields:

$$\varepsilon^0 : D_0^2 u_0 + \omega_0^2 u_0 = 0 \tag{7a}$$

$$\varepsilon^1 : D_0^2 u_1 + \omega_0^2 u_1 = -\left(2D_o D_1 u_0 + 6\eta u_0 \left(D_0 u_0\right)^2 + 3\eta {u_0}^2 {D_0}^2 u_0 + \omega_0^2 {u_0}^3 + \mu D_0 u_0 + \mu\beta\delta\left(D_0 u_0\right)^3\right) \tag{7b}$$

A general solution of Eq. (7a) is:

$$u_0 = A(T_1)e^{i\omega_0 T_0} + \overline{A}(T_1)e^{-i\omega_0 T_0} = a\cos(\omega_0 T_0 + \theta) \tag{8}$$

where *A* is a complex function of T_1 and $\overline{A}$ denotes complex conjugate of *A*. Substituting Eq. (8) into Eq. (7b) and eliminating the secular terms leads to:

$$2i\omega_0 A' + 3{\omega_0}^2(1-\eta)A^2\overline{A} + i\mu\omega_0 A + 3i\mu\beta\delta A^2\overline{A}{\omega_0}^3 = 0 \tag{9}$$

where in the above equation and rest of the paper prime denotes derivative with respect to T_1. It is convenient to write *A* in polar form as:

$$A = \frac{1}{2}ae^{i\theta} \tag{10}$$

where a and θ are real quantities. Substituting Eq. (10) into Eq. (9) and separating the real and imaginary parts yields:

$$\mathrm{Re} : \frac{3}{8}a^3{\omega_0}^2(\eta - 1) + a\omega_0\theta' = 0 \tag{11a}$$

$$\mathrm{Im} : \omega_0 a' + \frac{\mu}{2}\omega_0 a + \frac{3}{8}\mu\beta\delta{\omega_0}^3 a^3 = 0 \tag{11b}$$

The solution of Eq. (11a) is:

$$a = \sqrt{\left[\frac{4\mu}{8e^{-\mu(B-T_1)} - 3\mu\beta\delta\omega_0^2}\right]} \tag{12}$$

Substitution of Eq. (12) into Eq. (11b) leads to:

$$\theta = \frac{(1-\eta)\left[Ln\left(8e^{-\mu(B-T_1)} - 3\mu\beta\delta\omega_0^2\right) - \mu T_1\right]}{2\mu\beta\delta\omega_0} + \theta_0 \tag{13}$$

and θ_0 are constants. By substitution of Eqs. (12) and (13) into Eq. (8) one obtains:

$$u_0 = \sqrt{\left[\frac{4\mu}{8e^{-\mu(B-T_1)} - 3\mu\beta\delta\omega_0^2}\right]} \cos\left[\omega_0 t + \frac{(1-\eta)\left[Ln\left(8e^{-\mu(B-T_1)} - 3\mu\beta\delta\omega_0^2\right) - \mu T_1\right]}{2\mu\beta\delta\omega_0} + \theta_0\right] \tag{14}$$

3.2 Numerical Solution

Numerical integration of Eq. (3) is carried out by the 4th-order Runge-Kutta method. Numerical solutions for different initial conditions such as $u(0) = 0.5, u(0) = 1, u(0) = 2$ with $\dot{u}(0) = 0$ are obtained and compared with their analytical solutions, Eq.(14). Results are obtained with $m = 1$, $\varepsilon = 0.5$, $c_2 = c_3 = 2$ and $\xi = 0.1,1$ which shows different levels of system nonlinearities.

From Fig.2 and Fig.3 it can be observed that for $0.1 \le \xi \le 1$ and $u(0) \le 1$, the numerical and analytical solutions are in good agreement. Fig. 4 shows that by increasing the damping coefficient μ, the deflection of the nonlinear spring reduces faster. Fig. 5 shows that increasing the non-dimensional damping ratio β reduces the deflection of nonlinear spring. It can also be noted that the linear damping coefficient μ can reduce system response more effectively.

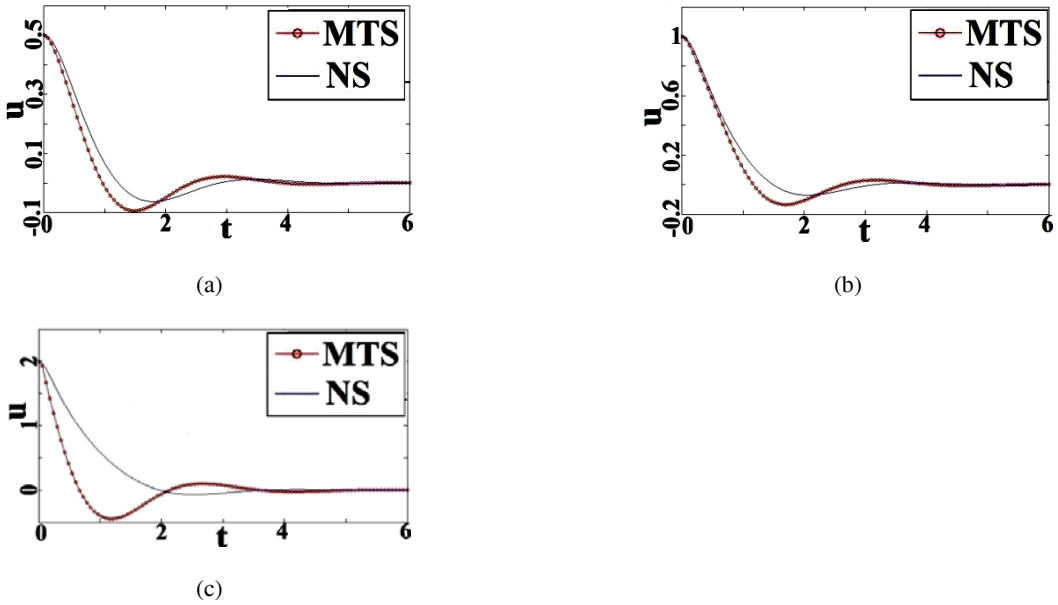

Fig. 2
Deflection of the nonlinear spring u with time for $\varepsilon = 0.5$, $c_2 = c_3 = 2$, $\xi = 0.1$ ($k_1 = 50, k_2 = 5$), $\eta = 0.0909, \omega_0 = 2.132$. (a) u(0)=0.5, (b) u(0)=1, (c) u(0)=2.

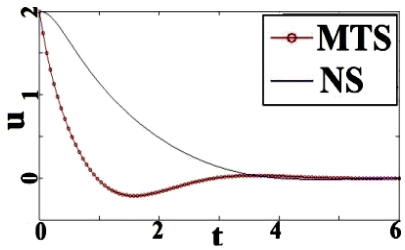

(a)

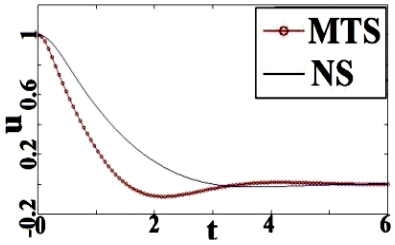

(b)

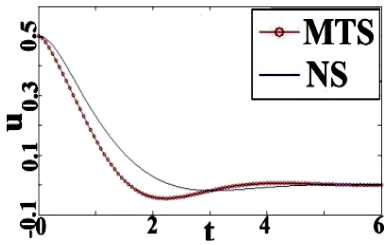

(c)

Fig. 3
Deflection of the nonlinear spring *u* with time for $\varepsilon = 0.5$, $c_2 = c_3 = 2$, $\xi = 1(k_1 = k_2 = 5)$, $\eta = 0.5, \omega_0 = 1.5811$. (a) u(0)=0.5, (b) u(0)=1, (c) u(0)=2.

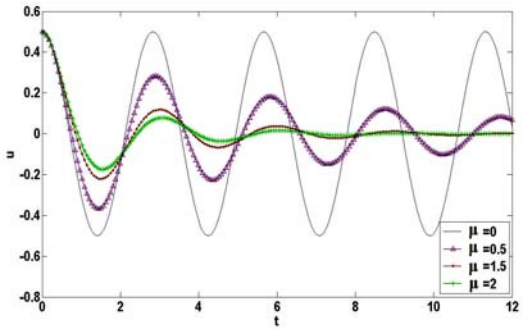

Fig. 4
Variations of deflection of the nonlinear spring *u* with time for different *v* alues of μ and $\varepsilon = 0.5$, $\xi = 0.1(k_1 = 50, k_2 = 5)$, $\eta = 0.909, \omega_0 = 2.132, \beta = 1.$

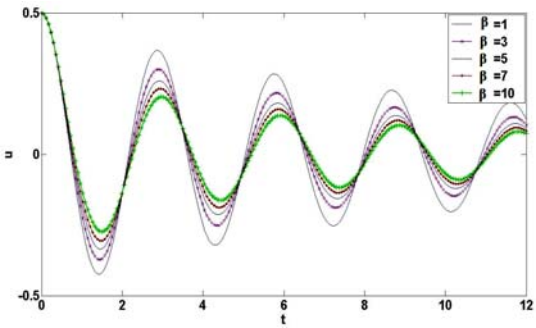

Fig. 5
Variations of deflection of the nonlinear spring *u* with time for different values of β and $\varepsilon = 0.5, \xi = 0.1(k_1 = 50, k_2 = 5)$, $\eta = 0.909, \omega_0 = 2.132, \mu = 0.25.$

4 FORCED VIBRATIONS

Let an external harmonic excitation *P*(*t*) be exerted to the mass of the system as:

$$P(t) = P\cos(\Omega t) \tag{15}$$

Equation of motion is derived as:

$$\ddot{u} + \varepsilon\mu\dot{u} + {\omega_0}^2 u + \varepsilon(6\lambda\eta u\dot{u}^2 + 3\lambda\eta u^2\ddot{u} + \lambda{\omega_0}^2 u^3 + \mu\beta\delta\dot{u}^3) = P\cos(\Omega t) \tag{16}$$

Two types of excitations, primary and secondary resonances (hard excitations) will be discussed here and the effects of the system parameters on the frequency-response will be investigated.

4.1 Primary resonance

In this case, it is assumed that the frequency of excitation, Ω is close to the linear frequency of the system, ω_0. A detuning parameter σ is used to show closeness of Ω to ω_0 as:

$$\Omega = \omega_0 + \varepsilon\sigma \tag{17}$$

To obtain a uniformly valid approximate solution, the excitation must be in the same order of nonlinear terms. So in Eq. (16) excitation amplitude is considered as:

$$P = \varepsilon P_0 \tag{18}$$

Multiple time scales method is used to solve equations of motion (16). The two term expansion of *u* in MTS method is used as [7]:

$$u = u_0 + \varepsilon u_1 \tag{19}$$

Substituting Eqs. (18), (19) and (6) into Eq. (16) and separating the same coefficients of ε^0 and ε^1 yields:

$$\varepsilon^0 : D_0^2 u_0 + \omega_0^2 u_0 = 0 \tag{20a}$$

$$\varepsilon^1 : D_0^2 u_1 + \omega_0^2 u_1 = -\begin{pmatrix} 2D_o D_1 u_0 + 6\lambda\eta u_0 \left(D_0 u_0\right)^2 + 3\lambda\eta u_0^2 {D_0}^2 u_0 + \lambda\omega_0^2 {u_0}^3 + \mu D_0 u_0 \\ +\mu\beta\delta(D_0 u_0)^3 - P_0\cos\left(\Omega T_0\right) \end{pmatrix} \tag{20b}$$

To determine secular terms in Eq. (20b), the excitation term can be written as:

$$P_0\cos\left(\Omega T_0\right) = \frac{P_0}{2}\left(e^{i\Omega T_0} + e^{-i\Omega T_0}\right) = \frac{P_0}{2}\left(e^{i\left(\omega_0 T_0 + \sigma T_1\right)} + e^{-i\left(\omega_0 T_0 + \sigma T_1\right)}\right) \tag{21}$$

A general solution of Eq. (20a) is:

$$u_0 = A(T_1)e^{i\omega_0 T_0} + \overline{A}(T_1)e^{-i\omega_0 T_0} \tag{22}$$

where *A* is a complex function of T_1 and $\overline{A}$ is the complex conjugate of *A*. Substituting Eqs. (21) and (22) into Eq. (20b) and eliminating the secular terms leads to:

$$2i\omega_0 A' + 3\lambda{\omega_0}^2(1-\eta)A^2\overline{A} - \frac{1}{2}P_0 e^{i\sigma T_1} + i\mu\omega_0 A + 3i\mu\beta\delta A^2\overline{A}{\omega_0}^3 = 0 \tag{23}$$

Substituting the polar form of Eq. (10) into Eq. (23) and separating the real and imaginary parts yields:

$$\mathrm{Im}: \omega_0 a' - \frac{1}{2} P_0 \sin(\sigma T_1 - \theta) + \frac{\mu}{2} \mu\omega_0 a + \frac{3}{8} \mu\beta\delta {\omega_0}^3 a^3 = 0 \tag{24a}$$

$$\mathrm{Re}: a\omega_0 \theta' - \frac{3}{8} \lambda a^3 {\omega_0}^2 (1-\eta) + \frac{1}{2} P_0 \cos(\sigma T_1 - \theta) = 0 \tag{24b}$$

The term T_1 can be eliminated by transforming Eq. (24) to an autonomous system considering:

$$\alpha = \sigma T_1 - \theta \tag{25}$$

Substituting Eq. (25) into Eq. (24) leads to:

$$a' = \frac{1}{2} \frac{P_0}{\omega_0} \sin\alpha - \frac{1}{2} \mu a - \frac{3}{8} \mu\beta\delta a^3 {\omega_0}^2 \tag{26a}$$

$$\alpha a' = \frac{1}{2} \frac{P_0}{\omega_0} \cos\alpha + a\sigma + \frac{3}{8} \lambda a^3 \omega_0 (\eta - 1) \tag{26b}$$

The point at which $a' = 0$ and $\alpha' = 0$ corresponds to the singular point of the system that shows the steady-state motion [7]. The steady-state condition may be given as:

$$P_0 \sin\alpha - \frac{3}{4} \mu\beta\delta a^3 {\omega_0}^3 - \omega_0 \mu a = 0 \tag{27a}$$

$$P_0 \cos\alpha - \frac{3}{4} \lambda \omega_0^2 a^3 (1-\eta) + 2\sigma\omega_0 a = 0 \tag{27b}$$

Using Eqs. (27a) and (27b), the frequency-response equation is obtained as:

$$P_0^2 = \left[\frac{3}{4} \mu\beta\delta a^3 {\omega_0}^3 + \omega_0 \mu a \right]^2 + \left[\frac{3}{4} \lambda {\omega_0}^2 a^3 (1-\eta) - 2\sigma\omega_0 a \right]^2 \tag{28}$$

Eq. (28) shows the relation between parameters $P_0, \lambda, a, \eta, \mu, \beta, \delta$ and σ in the steady-state solution.

Fig. 6 shows the effects of the parameters λ, η, P, μ and β on the steady state-amplitude against the detuning parameter σ.

4.2 Super-harmonic resonance

When Ω is away from ω_0, the excitation will have small effect unless its amplitude is hard. So in this case *P* is considered of order one [7]. A detuning parameter is introduced to show closeness of Ω and $\frac{1}{2}\omega_0$ as:

$$3\Omega = \omega_0 + \varepsilon\sigma \tag{29}$$

Applying MTS method in Eq. (16) and separating the terms with the same orders of ε as discussed before, one obtains:

$$\varepsilon^0 : D_0^2 u_0 + \omega_0^2 u_0 = P\cos(\Omega T_0) \tag{30a}$$

$$\varepsilon^1 : D_0^2 u_1 + \omega_0^2 u_1 = -\left(2D_o D_1 u_0 + 6\lambda\eta u_0 (D_0 u_0)^2 + 3\lambda\eta u_0^2 {D_0}^2 u_0 + \lambda\omega_0^2 {u_0}^3 + \mu D_0 u_0 + \mu\beta\delta (D_0 u_0)^3 \right) \tag{30b}$$

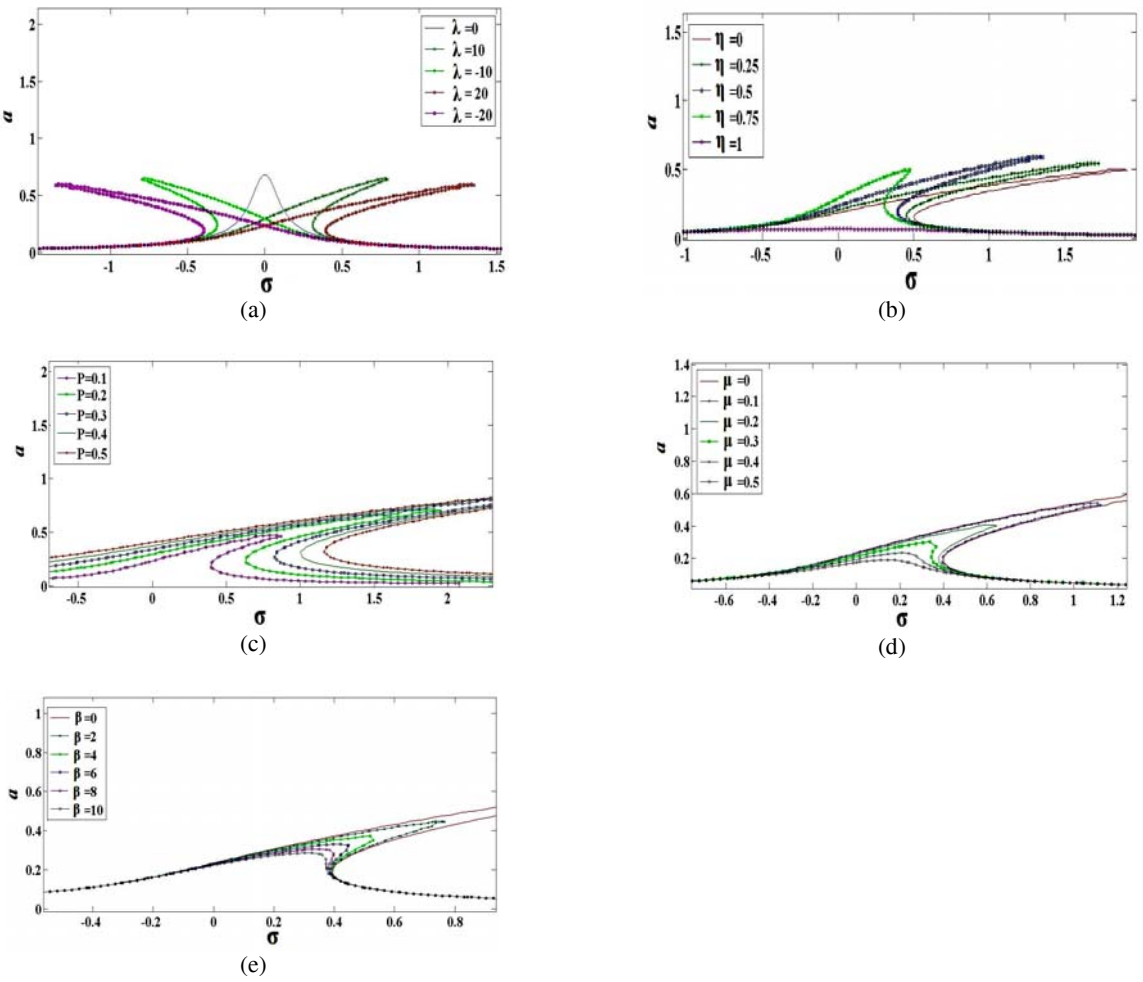

Fig. 6
Effects of the system parameters on the amplitude with respect to the detuning parameter σ for $\omega_0 = 1$, (a) effects of nonlinearity for $\eta = 0.5, P = 0.1, \mu = 0.1, \beta = 3$, (b) effects of η for $\lambda = 20, P = 0.1, \mu = 0.1, \beta = 3$, (c) effects of the amplitude of excitation for $\lambda = 20, \eta = 0.5, \mu = 0.1, \beta = 3$, (d) effects of μ for $\lambda = 20, P_0 = 0.1, \eta = 0.5, \beta = 3$, (e) effects of β for $\lambda = 20, P_0 = 0.1, \eta = 0.5, \mu = 0.1$.

The solution of Eq. (30a) can be expressed as:

$$u_0 = A(T_1)e^{i\omega_0 T_0} + \overline{A}(T_1)e^{-i\omega_0 T_0} + \tau(e^{i\Omega T_0} + e^{-i\Omega T_0}) \tag{31}$$

where $\tau = \dfrac{P}{2(\omega_0{}^2 - \Omega^2)}$ is a real parameter and A will be determined by eliminating the secular terms. Substituting Eqs. (29) and (31) into Eq. (30b) and eliminating the secular terms gives:

$$\begin{aligned} &2i\omega_0 A' + 3\lambda\omega_0{}^2(1-\eta)A^2\overline{A} + 6\lambda\eta\omega_0{}^2\tau^2(1-\eta)A + i\mu\omega_0 A + (\omega_0{}^2 - 9\eta\Omega^2)\lambda\tau^3 e^{i\sigma T_1} \\ &+ i\mu\beta\delta(3A^2\overline{A}\omega_0{}^3 + 6A\Omega^2\tau^2\omega_0 - \Omega^3\tau^3 e^{i\sigma T_1}) = 0 \end{aligned} \tag{32}$$

Using Eq. (10) and separating the real and imaginary parts of Eq. (32) leads to:

$$\mathrm{Im}: \omega_0 a' + \frac{\mu}{2}\omega_0 a + \frac{3}{8}\mu\beta\delta{\omega_0}^3 a^3 + 3\mu\beta\delta a\tau^2\Omega^2\omega_0 - \mu\beta\delta\tau^3\Omega^2\cos(\sigma T_1 - \theta) + ({\omega_0}^2 - 9\eta\Omega^2)\lambda\tau^3\sin(\sigma T_1 - \theta) = 0 \tag{33a}$$

$$\mathrm{Re}: -\omega_0 a\theta' + \frac{3}{8}\lambda{\omega_0}^2 a^3(1-\eta) + 3\lambda{\omega_0}^2\tau^2(1-\eta)a + \mu\beta\delta\tau^3\Omega^2\sin(\sigma T_1 - \theta) + ({\omega_0}^2 - 9\eta\Omega^2)\lambda\tau^3\cos(\sigma T_1 - \theta) = 0 \tag{33b}$$

Eq. (33) is transformed to an autonomous system by introducing a new variable as:

$$\alpha = \sigma T_1 - \theta \tag{34}$$

Therefore

$$a' = (9\eta\frac{\Omega^2}{\omega_0} - \omega_0)\lambda\tau^3\sin(\alpha) - \frac{\mu}{2}a - \frac{3}{8}\mu\beta\delta{\omega_0}^2 a^3 - 3\mu\beta\delta a\tau^2\Omega^2 + \mu\beta\delta\tau^3\frac{\Omega^2}{\omega_0}\cos(\alpha) \tag{35a}$$

$$a\alpha' = (9\eta\frac{\Omega^2}{\omega_0} - \omega_0)\lambda\tau^3\cos(\alpha) + a\sigma + \frac{3}{8}\lambda\omega_0 a^3(\eta - 1) + 3\lambda\omega_0\tau^2(\eta - 1)a - \mu\beta\delta\tau^3\Omega^2\sin(\alpha) \tag{35b}$$

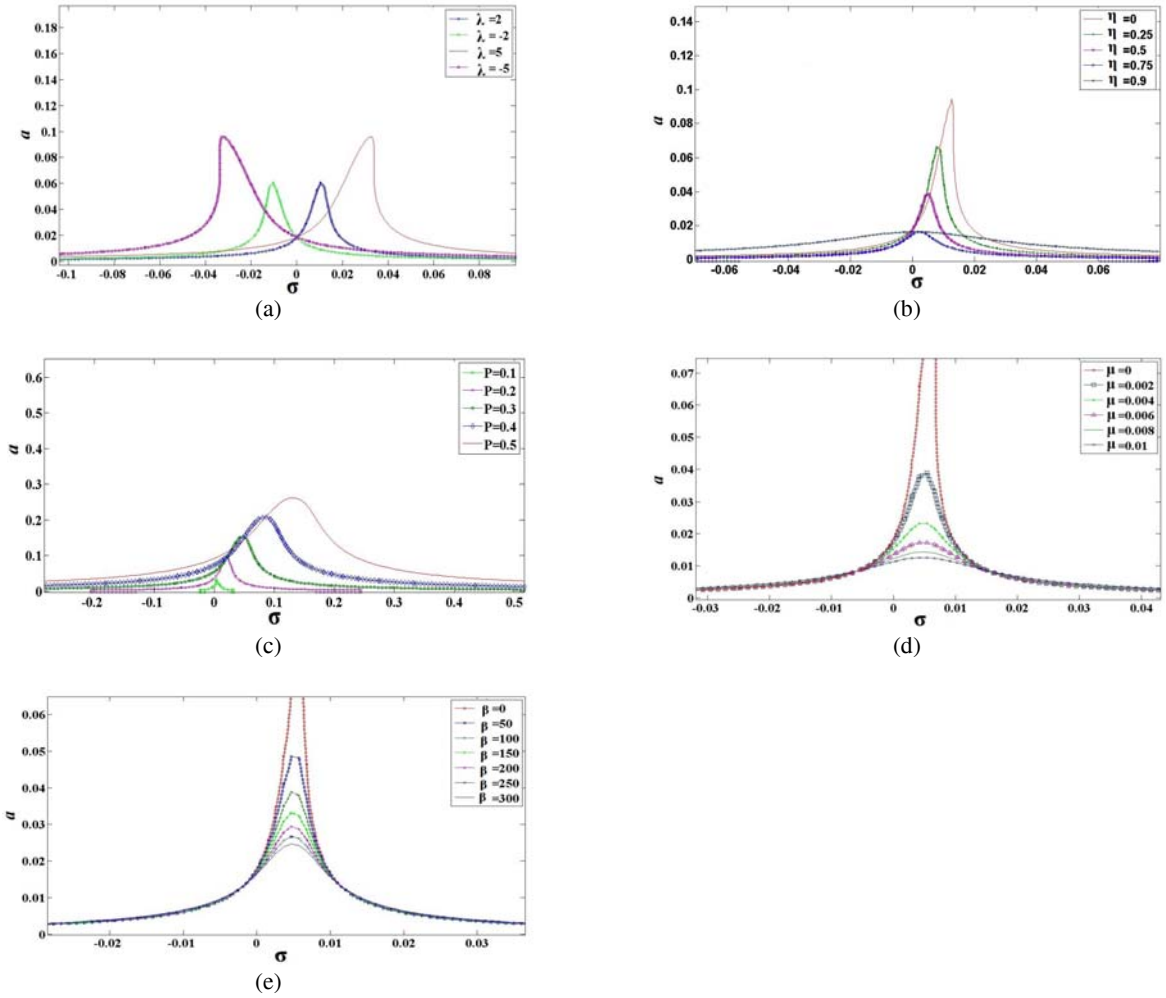

Fig. 7

Effects of system parameters on the amplitude with respect to the detuning parameter σ for ω_0 = 1, (a) effects of nonlinearity for $\eta = 0.5, P = 0.1, \mu = 0.002, \beta = 100$, (b) effects of η for $\lambda = 1, P = 0.1, \mu = 0.002, \beta = 100$, (c) effects of amplitude of excitation for $\eta = 0.5, \lambda = 1, \mu = 0.002, \beta = 100$, (d) effects of μ for $\eta = 0.5, \lambda = 1, P = 0.1, \beta = 100$, (e) effects of β for $\eta = 0.5, \lambda = 1, P = 0.1, \mu = 0.002$.

The frequency-response equation corresponding to the steady-state motion is obtained as:

$$\left[\frac{3}{8}\lambda\omega_0^2(1-\eta)a^3 - a\sigma\omega_0 + 3\lambda\omega_0^2\tau^2(1-\eta)a\right]^2 + \left[\frac{1}{2}\mu a\omega_0 + \frac{3}{8}\mu\beta\delta a^3\omega_0^3 + \tau^2\Omega^2\omega_0\right]^2 = \left[\left(9\eta\Omega^2 - \omega_0^2\right)\lambda\tau^3\right]^2 + \left[\mu\beta\delta\tau^3\Omega^2\right]^2 \tag{36}$$

Fig. 7 illustrates the effects of system parameters on the steady state amplitude of the system.

4.3 Sub-harmonic resonance

The sub-harmonic resonance occurs when Ω is near $3\omega_0$. The detuning parameter σ is introduced as:

$$\Omega = 3\omega_0 + \varepsilon\sigma \tag{37}$$

The same as the super-harmonic resonant case, by substituting Eq. (37) into Eq. (30) and separating the terms proportional to $e^{\pm i\omega_0 T_0}$, the solvability condition is obtained as:

$$2i\omega_0 A' + 3\lambda\omega_0^2(1-\eta)A^2\overline{A} + 6\lambda\omega_0^2\tau^2(1-\eta)A + i\mu\omega_0 A + \lambda\tau\left[12\eta(\Omega\omega_0 - \omega_0^2) + 3(\omega_0^2 - \eta\Omega^2)\right]\overline{A}^2 e^{i\sigma T_1} + 3\mu\beta\delta(iA^2\overline{A}\omega_0^3 + 2iA\Omega^2\tau^2\omega_0 - i\overline{A}^2\Omega\tau\omega_0^2 e^{i\sigma T_1}) = 0 \tag{38}$$

where $\tau = \dfrac{P}{2(\omega_0^2 - \Omega^2)}$. Letting A in polar form as Eq. (10) and separating the real and imaginary parts of the derived equation yields:

$$\mathrm{Im}: \omega_0 a' + \frac{\mu}{2}\omega_0 a + \frac{3}{8}\mu\beta\delta\omega_0^3 a^3 + 3\mu\beta\delta a\tau^2\Omega^2\omega_0 + \frac{3}{4}\mu\beta\delta\tau\Omega\omega_0^2 a^2\cos(\sigma T_1 - 3\theta) + \frac{1}{4}\left[12\eta(\Omega\omega_0 - \omega_0^2) + 3(\omega_0^2 - \eta\Omega^2)\right]\lambda\tau a^2\sin(\sigma T_1 - 3\theta) = 0 \tag{39a}$$

$$\mathrm{Re}: -\omega_0 a\theta' + \frac{3}{8}\lambda\omega_0^2 a^3(1-\eta) + 3\lambda\omega_0^2\tau^2(1-\eta)a + \frac{3}{4}\mu\beta\delta\tau\Omega\omega_0^2 a^2\sin(\sigma T_1 - 3\theta) + \frac{1}{4}\left[12\eta(\Omega\omega_0 - \omega_0^2) + 3(\omega_0^2 - \eta\Omega^2)\right]\lambda\tau a^2\cos(\sigma T_1 - 3\theta) = 0 \tag{39b}$$

Eq.(39) is transformed to an autonomous system using:

$$\alpha = \sigma T_1 - 3\theta \tag{40}$$

In the steady-state motion, $\alpha' = 0$ and $\alpha' = 0$ and the frequency-response in this case will be:

$$\left[\frac{3}{8}\lambda\omega_0^2(\eta-1)a^3 + 3\lambda\omega_0^2\tau^2(\eta-1)a + \frac{1}{3}\omega_0 a\sigma\right]^2 + \left[\frac{1}{2}\mu\omega_0 a + \frac{3}{8}\mu\beta\delta\omega_0^3 a^3 + 3\mu\beta\delta\Omega^2\tau^2\omega_0 a\right]^2 = \left[\frac{1}{4}\lambda\tau\left[12\eta\left(\Omega\omega_0 - \omega_0^2\right) + 3(\omega_0^2 - \eta\Omega^2)\right]a^2\right]^2 + \left[\frac{3}{4}\mu\beta\delta\omega_0^2\tau\Omega a^2\right]^2 \tag{41}$$

The amplitudes of the system against the detuning parameter σ are shown in Figs. (8) - (10) for different system parameters.

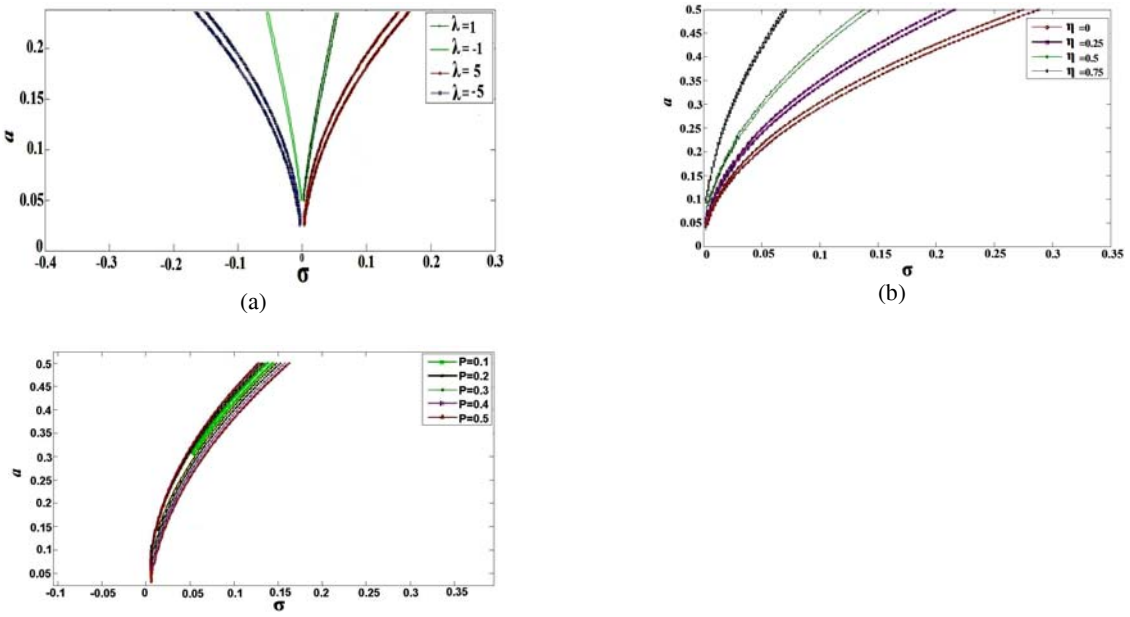

(a) (b)

(c)

Fig. 8

Effects of system parameters on the amplitude with the detuning parameter σ for ω_0 = 1, (a) effects of nonlinearity parameter for $\eta = 0.5, P = 0.1, \mu = 0.0002, \beta = 3$, (b) effects of η for $\lambda = 1, P = 0.1, \mu = 0.0002, \beta = 3$, (c) effects of amplitude of excitation for $\eta = 0.5, \lambda = 1, \mu = 0.0002, \beta = 3$.

(a) (b)

Fig. 9

Effects of μ on the amplitude for $\eta = 0.5, \lambda = 1, P = 0.1, \beta = 3$, $(a)\mu = 0.0002, (b)\mu = 0.001.$

(a) (b)

Fig. 10

Effects of β on the amplitude for $\eta = 0.5, \lambda = 1, P = 0.1, \mu = 0.0002$, $(a)\beta = 0, (b)\beta = 5.$

5 BIFURCATION ANALYSIS

In section 4, equation of motion of the system with nonlinear damper under a harmonic load is given in Eq. (16). By defining state variables as $u = x$ and $\dot{u} = y$, Eq. (16) can be written as:

$$\begin{cases} \dot{x} = y \\ \dot{y} = \dfrac{P\cos(\Omega t) - \omega_0{}^2 x - \varepsilon\left[6\lambda\eta x y^2 + \lambda\omega_0{}^2 x^3 + \mu\beta\delta y^3 + \mu y\right]}{1 + 3\varepsilon\lambda\eta x^2} \end{cases} \tag{42}$$

In Eq. (42), the controlling parameters are P, η, μ, β and the other parameters are set as $\Omega = 3, \varepsilon = 0.5, \lambda = 20,$ $\omega_0 = 1$. The 4th-order Runge-Kutta method is used to solve Eq. (42).

5.1 Effects of the controlling parameter P on the system behavior

In order to investigate the effect of excitation parameter *P* on the system behavior, we assume $\eta = 0.5, \mu = 0.1$ and $\beta = 5$. Bifurcation and phase diagrams, and Poincare map are used to study this case. Fig.11 shows bifurcation diagram for the displacement *u* in terms of the controlling parameter *P* for $0.5 \le P \le 1.3$. When $P \in [0.5, 0.625]$, the graph has only one branch which indicates the system has a periodic motion with time period *T*. At *P*= 0.63 which is a bifurcation point, the response bifurcates into three branches where the two lower branches are very close. For $P \in [0.63, 0.66]$ a 3*T* periodic motion is anticipated. At *P*= 0.66, the three branches merge into one branch. When $P \in [0.66, 0.8]$, there is only one branch that relates to a periodic motion with period *T*. Furthermore, for $P \in [0.94, 1.17]$, the system will have quasi-periodic or chaotic behavior.

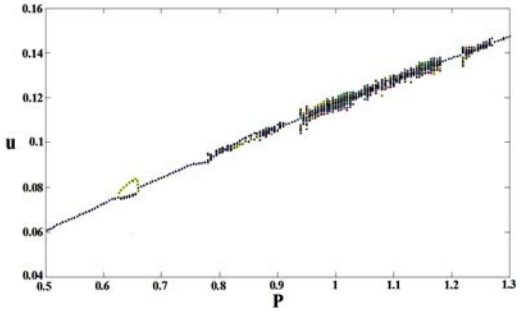

Fig. 11
Bifurcation diagram for the controlling parameter *P*.

Fig. 12 shows phase diagram and Poincare map for *P*= 0.6 where the system has periodic motion with period *T*. For *P*=0.65, the system will commence a periodic motion with period 3*T*, as can be seen in phase diagram and Poincare map shown in Fig. 13. With the controlling parameter *P*=0.95, as shown in Fig. 14, the system behavior will transform from periodic to quasi-period motion.

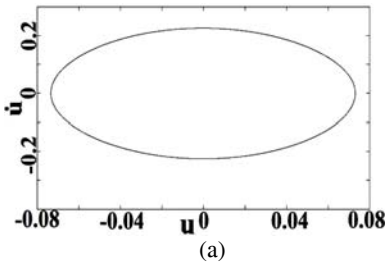

(a)

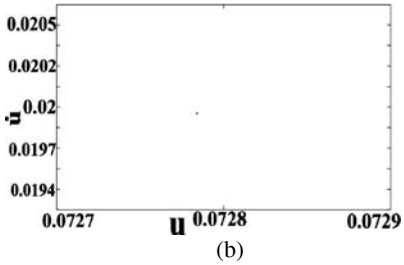

(b)

Fig. 12
(a) Phase diagram, (b) Poincare map for the controlling parameter $P = 0.6$.

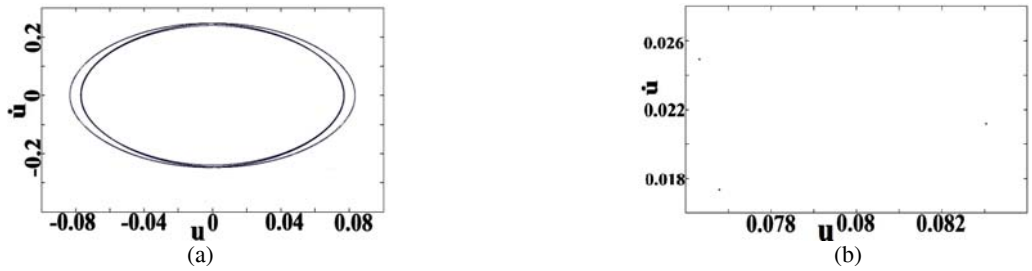

(a) (b)

Fig. 13
(a) Phase diagram, (b) Poincare map for the controlling parameter $P = 0.65$.

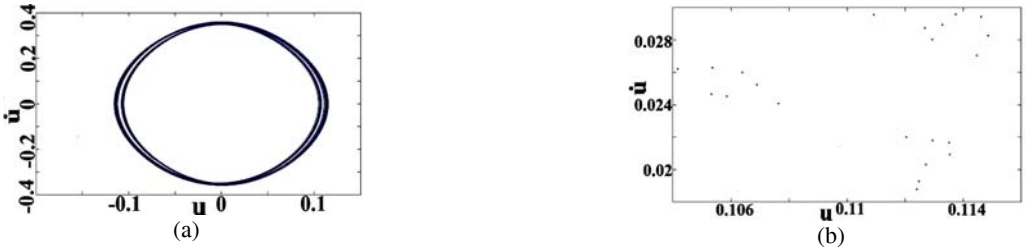

(a) (b)

Fig. 14
(a) Phase diagram, (b) Poincare map for the controlling parameter $P = 0.95$.

5. 2 Effects of the controlling parameter η *on the system behavior*

The effect of the controlling parameter η which is related to the linear parts of the spring stiffnesses, on the system behavior is investigated for $\beta = 5, \mu = 0.1, P = 0.5$. In this case, bifurcation and phase diagrams and Poincare map are plotted.

Fig. 15 shows displacement u in terms of the controlling parameter η for $0 \le \eta \le 0.4$. It is observed that when $0 \le \eta \le 0.3$, the number of equilibrium points are limited and the system has periodic behavior. For $\eta \ge 0.3$, rapid increase of equilibrium points occurs and the system behavior transforms to chaotic motion. When $\eta \in [0, 0.065]$ and $\eta \in [0.065, 0.19]$ the system behavior is $3T$ periodic and quasi-periodic, respectively. In the range of $\eta \in [0.19, 0.255]$, a periodic motion with one equilibrium point exists and at $\eta = 0.255$ the graph branches into two. For $\eta \in [0.255, 0.3]$ the graph has two branches representing a periodic motion with period $2T$.

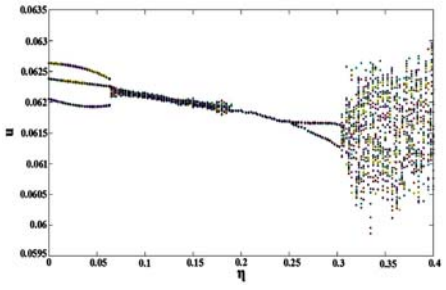

Fig. 15
Bifurcation diagram for the controlling parameter η.

Fig. 16 shows phase diagram and Poincare map for the controlling parameter $\eta = 0.03$. Since the Poincare map has three points in phase space, the system has a periodic motion with $3T$ period. With increasing η, the number of

equilibrium points and the system period increase as well. For $\eta = 0.18$, as shown in Fig. 17, the system has a periodic motion with 10T period. Fig. 18 Fig. 19 are plotted for $\eta = 0.2$ and $\eta = 0.27$, respectively. It may be seen that for $\eta = 0.2$ the period is *T* and for $\eta = 0.27$ the period is 2T. Fig. 20 that is plotted for $\eta = 0.365$ shows that increasing η beyond 0.3 results in chaotic motion of the system.

(a) (b)

Fig. 16
(a) Phase diagram, (b) Poincare map for the controlling parameter $\eta = 0.03$.

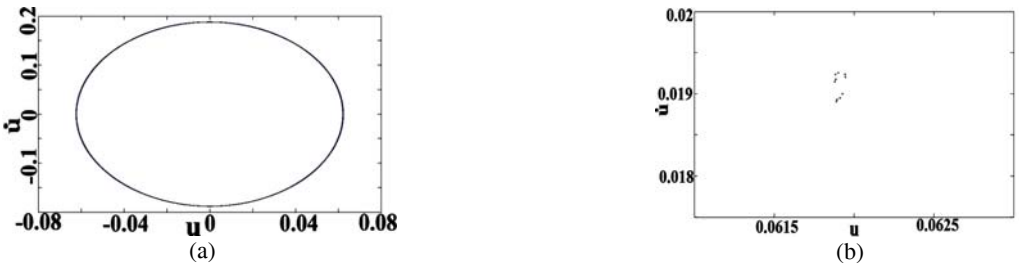

(a) (b)

Fig. 17
(a) Phase diagram, (b) Poincare map for the controlling parameter $\eta = 0.18$.

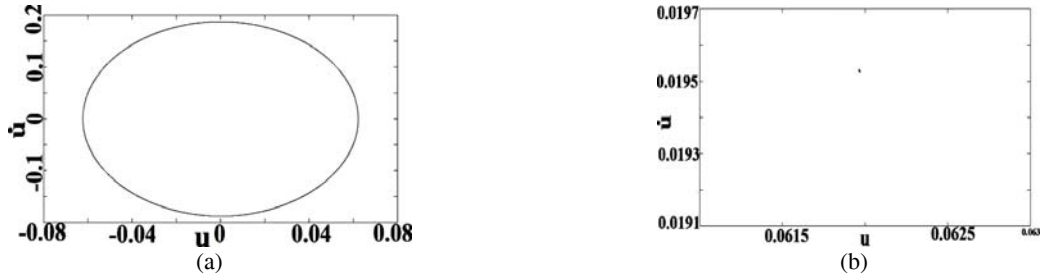

(a) (b)

Fig. 18
(a) Phase diagram, (b) Poincare map for the controlling parameter $\eta = 0.2$.

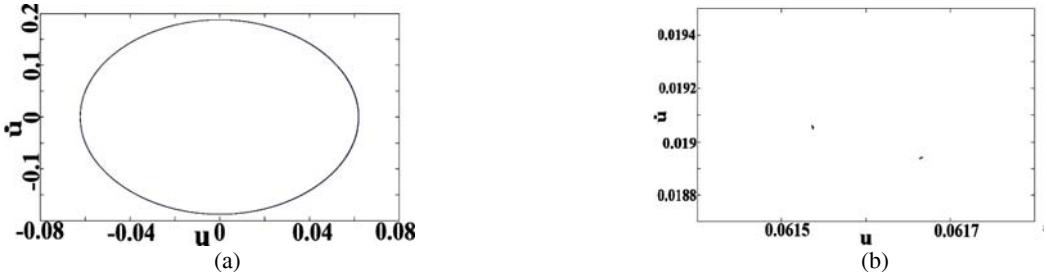

(a) (b)

Fig. 19
(a) Phase diagram, (b) Poincare map for the controlling parameter $\eta = 0.27$.

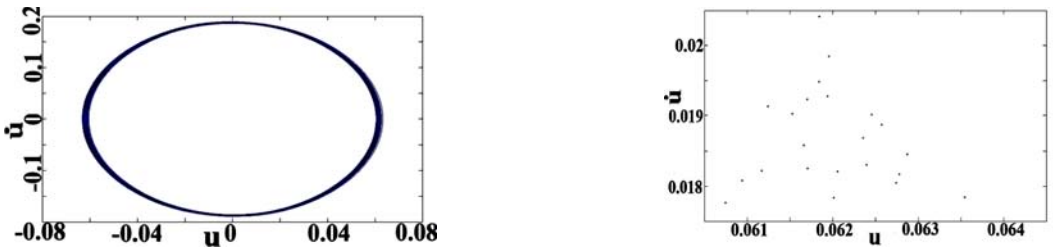

(a) (b)

Fig. 20
(a) Phase diagram, (b) Poincare map for the controlling parameter $\eta = 0.365$.

5.3 Effects of the controlling parameter μ on the system behavior

In this section, the effect of the controlling parameter μ which is a representative of the linear damping coefficient on the system behavior is investigated. For this case, the parameters are assumed as: $P = 0.65, \eta = 0.5, \beta = 5$.

Fig.21 illustrates bifurcation diagram of *u* in terms of the controlling parameter μ for $0 \le \mu \le 0.4$. It can be seen that for $\mu \in [0, 0.015]$ there are multi-equilibrium points. An increase in μ is accompanied by a decrease in the number of equilibrium points. For $\mu \in [0.015, 0.11]$, three branches exist. Thus, in this range of the controlling parameter, a periodic motion with 3T period is anticipated. At $\mu = 0.11$, the three branch diagram transforms to one branch and beyond this point, the system has only one equilibrium point. Therefore, in this range, a periodic motion with period *T* is expected.

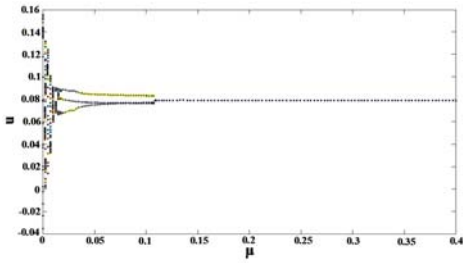

Fig. 21
Bifurcation diagram for the controlling parameter μ.

In Fig. 22, phase diagram and Poincare map are plotted for the controlling parameter $\mu = 0.01$. Since Poincare map includes points that produce a closed curve, for $\mu = 0.01$ the system has a quasi-periodic motion. Phase diagram confirm such motion. With the increase of μ, the number of system equilibrium points decreases and at $\mu = 0.03$ the system changes from quasi-periodic motion to a periodic motion with a period of 3*T*. Fig. 23 illustrates system diagrams for $\mu = 0.03$. Fig. 24 shows that for $\mu = 0.2$ the system has a periodic motion with period *T*. It may be concluded that with the increase of μ which is directly proportional to the linear damping coefficient, the system behavior transforms from a quasi-periodic to a periodic motion. This indicates the stabilizing effect of the system damping.

5. 4 Effects of the controlling parameter β on the system behavior

Effects of the controlling parameter β which is related to the nonlinear damping coefficient is studied for $P = 0.65, \eta = 0.5, \mu = 0.1$. Same as the previous cases, bifurcation diagram, phase diagram and Poincare map are used for the analyses.

Fig. 25 shows bifurcation of the displacement u in terms of the controlling parameter β for $0 \le \beta \le 15$. It can be seen that for $\beta \in [0, 5.4]$ the graph has three branches, so a periodic motion with a period $3T$ is predicted. At $\beta = 5.4$, the three branch graph transforms to one branch and beyond this point, the system has one equilibrium point that corresponds to a periodic motion with period T.

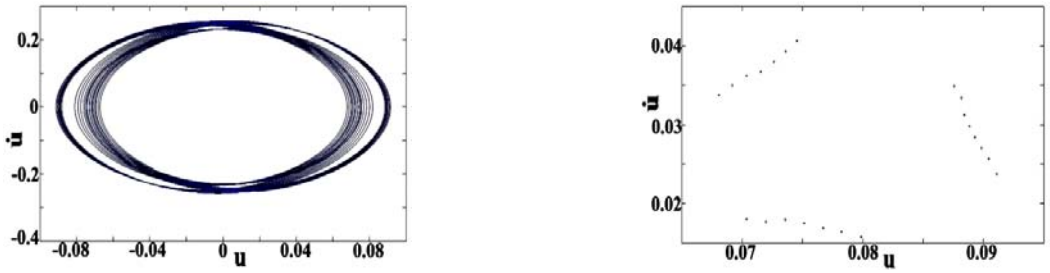

(a) (b)

Fig. 22
(a) Phase diagram, (b) Poincare map for the controlling parameter $\mu = 0.01$.

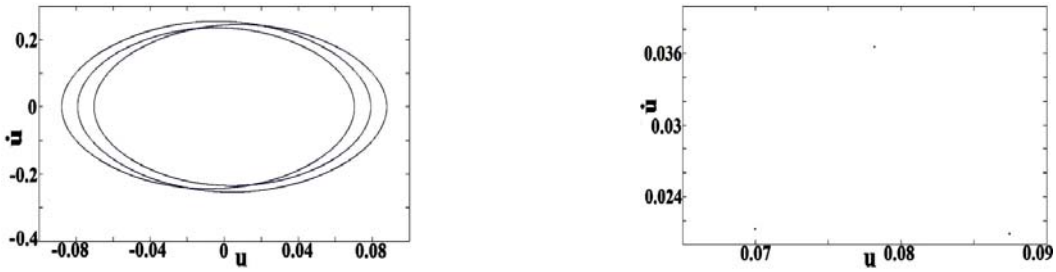

(a) (b)

Fig. 23
(a) Phase diagram, (b) Poincare map for the controlling parameter $\mu = 0.03$.

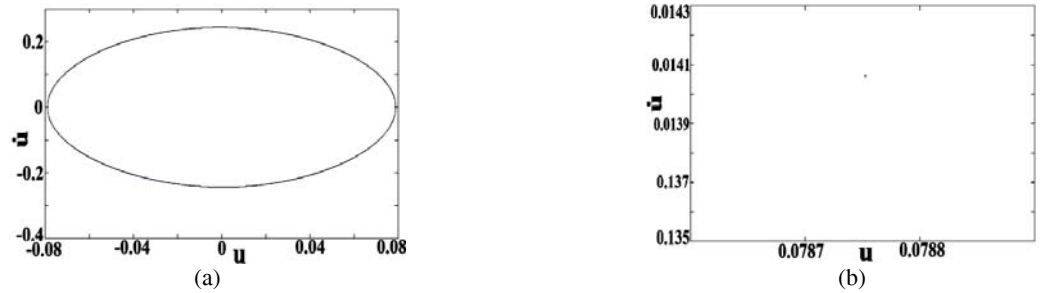

(a) (b)

Fig. 24
(a) Phase diagram, (b) Poincare map for the controlling parameter $\mu = 0.2$.

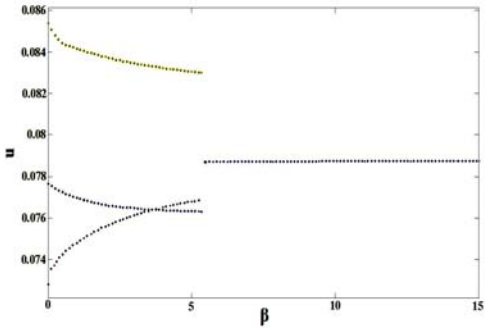

Fig. 25
Bifurcation for the controlling parameter β.

(a) (b)

Fig. 26
(a) Phase diagram, (b) Poincare Map for the controlling parameter $\beta = 1$.

(a) (b)

Fig. 27
(a) Phase diagram, (b) Poincare Map for the controlling parameter $\beta = 12$.

Fig. 26 shows phase diagram and Poincare map for $\beta = 1$. It may be seen that Poincare map includes three points, thus the system has periodic motion with a period 3*T*. Phase diagram confirms this behavior. Furthermore, with the increase of β, the number of the system equilibrium points decreases. Fig. 27 shows phase diagram and Poincare map for $\beta = 12$. The Poincare map includes one point and the phase diagram has a closed curve indicating a periodic motion with period *T*.

6 CONCLUSIONS

In this paper, vibration of a mass grounded by linear and nonlinear springs and a nonlinear damper is studied. In the first section, free vibration equation of the system is solved by MTS and numerical methods. It was shown that for $0.1 \le \xi \le 1$ and $u(0) \le 1$ the numerical solution is in good agreement with the approximate analytical solution. For

the forced vibrations, the amplitude-frequency equations of the system were derived for the primary, super-harmonic and sub-harmonic resonances using MTS method. At the final section, some parameters were considered as the controlling parameter and the bifurcation of the system response is investigated using phase diagrams and Poincare maps. The types of the system motions and the bifurcation points were identified.

REFERENCES

[1] Meirovitch L., 1975, *Elements of Vibration Analysis*, McGraw-Hill, New York.
[2] Dimarogonas A., 1996, *Vibration for Engineers*, Prentice-Hall, Englewood Cliffs, NJ.
[3] Telli S., Kopmaz O., 2006, Free vibrations of a mass grounded by linear and nonlinear springs in series, *Journal of Sound and Vibration* **289**:689-710.
[4] Sun W.P., Wu B.S., 2008, Large amplitude free vibrations of a mass grounded by linear and nonlinear springs in series, *Journal of Sound and Vibration* **314**:474-480.
[5] Wu B.S., Li P.S., 2001, A method for obtaining approximate analytic periods for a class of nonlinear oscillators, *Meccanica* **36**:167-176.
[6] Lai S.K., Lim C.W., 2007, Accurate approximate analytical solutions for nonlinear free vibration of systems with serial linear and nonlinear stiffness, *Journal of Sound and Vibration* **307**:720-736.
[7] Nayfeh A.H., Mook D.T., 1979, *Nonlinear Oscillations*, John Wiley & Sons Inc., New York.